A New Wave Breaking Criterion for a Finite Element Boussinesq Model

L. Pinheiro[1], C.J.E.M. Fortes[1], J.A. Santos[1,2], J. L. M. Fernandes[3], T. Okamoto[4]

[1]Laboratório Nacional de Engenharia Civil, NPE/DHA, Av. do Brasil, 101, 1700-066 Lisboa
e-mail: lpinheiro@lnec.pt, jfortes@lnec.pt, jasantos@lnec.pt http://www.dha.lnec.pt/npe/
[2]Instituto Superior de Engenharia de Lisboa, Rua Conselheiro Emídio Navarro 1, 1959-007, Lisboa
[3]Instituto Superior Técnico, Av. Rovisco Pais, 1 1049-001, Lisboa
4 Hiroshima University, Kagamiyama, Higashi-Hiroshima, Hiroshima, 739-8529, Japan

Summary

This paper describes the implementation and validation of two wave breaking methodologies in the BOUSS-WMH numerical model (BOUSSinesq Wave Modelfor Harbors). BOUSS-WMH is a finite element model for wave propagation based upon the extended Boussinesq equation derived by Nwogu [8].
In the present work, two empirical formulations were used: the first one is the well know and widespread using free surface elevation acceleration method and the other one is the newly developed that includes Relative Trough Froude Number. The two will be compared and their main advantages and disadvantages will be evaluated.

Key-Words: *Wave breaking, Wwave propagation, Boussinesq Equations, Finite Elements.*

1 INTRODUCTION

The numerical resolution of Boussinesq-type equations has been successfully accomplished with the finite element method that deals directly with unstructured grids and correctly represents the physical boundaries of the domain. (Antunes do Carmo and Seabra Santos [1], Li et al. [6], Walkley [17]; Walkley and Berzins [16]). Moreover the finite element method allows minimizing the number of points in the grid using local refinement techniques.

BOUSS-WMH model, Pinheiro *et al* [11], is a result of developments on Walkley and Berzins [16] model and now includes internal wave generation (using a source function method with which regular and irregular waves can be generated), artificial numerical viscosity (to control numerical instabilities), numerical sponge layers (placed on radiation boundaries to absorb outgoing waves), numerical porosity layers (placed either on physical boundaries or inside the domain to simulate the reflection, transmission and energy dissipation effects of porous structures on the waves) and energy dissipation due to bottom friction and wave breaking.

Several empirical formulations have been adopted by different authors to model wave breaking. In BOUSS-WMH wave breaking is modeled using the method proposed by Kennedy et al. [3]. In the present work, a new method of implementing wave breaking is added and is based on the work of and of Okamoto and Basco [10]. The two formulations will be compared and their main advantages and disadvantages will be evaluated.

This paper presents a general description of BOUSS-WMH model and the implementation of wave breaking using the two different formulations referred previously. The model is applied to two test cases for which experimental data is available, Hanssen and Svendsen [2], Sancho et al. [13] in order to validate the wave breaking formulations. First of all, the calibration of the wave breaking parameters for both formulations is made. Then, for the same test, different wave conditions are used and the behavior of wave breaking formulations is evaluated and compared. Statistical analysis is employed for a proper validation of the model.

2 NUMERICAL MODEL BOUSS3W

2.1 Basic equations

The extended Boussinesq equations derived by Nwogu [8] are given by the following equations, where the horizontal velocity vector $\mathbf{u} = \mathbf{u}(x, y, t) = (\mathrm{u}, \mathrm{v})$ is defined at depth $Z_\alpha = \theta_h$:

$$\frac{\partial \eta}{\partial t}+\nabla\left((h+\eta)\mathbf{u}\right)+\nabla\cdot\left(\left(\frac{Z_\alpha{}^2}{2}-\frac{h^2}{6}\right)h\nabla\left(\nabla\cdot\mathbf{u}\right)+\left(Z_\alpha+\frac{h}{2}\right)h\nabla\left(\nabla\cdot\left(h\mathbf{u}\right)\right)\right)=0 \tag{1}$$

$$\frac{\partial \boldsymbol{u}}{\partial t}+(\boldsymbol{u}\cdot\nabla)\boldsymbol{u}+g\nabla\eta+\frac{Z_\alpha{}^2}{2}\nabla\left(\nabla\cdot\frac{\partial \boldsymbol{u}}{\partial t}\right)+Z_\alpha\nabla\left(\nabla\cdot\left(h\frac{\partial \boldsymbol{u}}{\partial t}\right)\right)=0 \tag{2}$$

where η is the free surface elevation and *h* the water depth.

The original Nwogu's equations were further extended to take into account some important physical processes (wave transmission through porous structures, bottom friction and wave breaking) as well as other source/damping terms for numerical reasons. The BOUSS-WMH model equations result as follows:

$$\frac{\partial \eta}{\partial t}+\nabla\left((h+\eta)\mathbf{u}\right)+\nabla\cdot\left(\left(\frac{Z_\alpha{}^2}{2}-\frac{h^2}{6}\right)h\nabla\left(\nabla\cdot\mathbf{u}\right)+\left(Z_\alpha+\frac{h}{2}\right)h\nabla\left(\nabla\cdot\left(h\mathbf{u}\right)\right)\right)=S_f+\upsilon\nabla^2\eta \tag{3}$$

$$\frac{\partial \mathbf{u}}{\partial t}+(\mathbf{u}\cdot\nabla)\mathbf{u}+g\nabla\eta+\frac{Z_\alpha{}^2}{2}\nabla\left(\nabla\cdot\frac{\partial \mathbf{u}}{\partial t}\right)+Z_\alpha\nabla\left(\nabla\cdot\left(h\frac{\partial \mathbf{u}}{\partial t}\right)\right)=n\mathbf{u}\left(f_l+nf_t|\mathbf{u}|\right)+\frac{1}{h+\eta}\left(f_w\mathbf{u}|\mathbf{u}|+\nabla\upsilon_e\nabla(h+\eta)\mathbf{u}\right) \tag{4}$$

where the added terms stand for:

S_f - source function for wave generation;

$\upsilon\nabla^2\eta$ - viscous damping;

$n f_l \mathbf{u}+n f_t \mathbf{u}|\mathbf{u}|$ - laminar and turbulent friction (porous structures);

$\frac{1}{h+\eta} f_w \mathbf{u}|\mathbf{u}|$ - wave induced bottom friction;

$\frac{1}{h+\eta}\nabla\upsilon_e\nabla(h+\eta)\mathbf{u}$ - wave breaking.

The next sections will give some details about the added terms, in special, the one related with wave breaking.

2.2 Wave generation

The wave generation is made by an internal generation condition, which is added to the model, using a source function following the procedure described by Wei et al. [18]. In this method, the source function is derived by a linearized form of the Boussinesq equations and by using Green's theorem, an explicit relation between the desired surface wave amplitude and the source function amplitude is obtained.

2.3 Viscous damping

The viscous damping term has three components: The first component is distributed in time domain. The other two components are distributed in space domain. ν_t and ν_1 aim at controlling numerical instabilities while ν_2 aims at absorbing outgoing waves at fully absorptive boundaries.

$$\nu=\nu_t+\nu_1+\nu_2 \tag{5}$$

$$\nu_t=m_1\cdot e^{-m_2\frac{t}{T}},\ \nu_1=\frac{\gamma\cdot\lambda^4}{(2\cdot\pi\cdot\Delta x)^3}\ \text{and}\ \nu_2=\frac{30}{T}\cdot\frac{e^{\left(\frac{X-X_S}{X_F-X_S}\right)^2}-1}{e-1} \tag{6}$$

where T is the wave period (or Tm mean period for irregular waves) and m_1 and m_2 are empiric constants that usually range between $1\text{x}10^{-3}$ and $2\text{x}10^{-3}$ and 0.5 and 2, respectively, λ is the wave length, Δx is the average node spacing and γ is an empirical parameter in m/s that usually ranges between $2\text{x}10^{-6}$ and $8.5\text{x}10^{-6}$, XS is the starting location of the layer and XF is the final location of the layer. XF-XS is the width of the layer.

ν_t – In the first time steps this will damp the solution, allowing the use of larger time steps. Due to the exponential decay nature of this damping term, it will not affect the solution obtained after a suitably large time.

ν_1 – In order to avoid spurious modes that damp the numerical solution, a small viscosity is introduced equally distributed in space and covering the whole domain.

ν_2 – A viscous damping layer, termed sponge layer, is introduced near the outflow boundary in order to absorb incident waves at those boundaries. It was found in practice that the width of the sponge layer must be one to two wavelengths, in order to provide sufficient damping, Kirby et al. [4].

2.4 Bottom friction

The effect of energy dissipation due to a turbulent bottom boundary layer is simulated using a term of bottom shear stress, F_b, following the procedure adopted by Nwogu and Demirbilek [7]. The wave friction factor estimates the bottom shear stress induced by the passage of the wave. To estimate the wave friction factor the method presented by Le Roux [5] is used.

2.5 Wave breaking

Wave breaking is a very complex turbulent phenomenon that constitutes an important form of energy dissipation and cannot be neglected in near shore areas. Several empirical formulations have been adopted by different authors to model wave breaking. In the next section we refer to the eddy viscosity approach to model energy dissipation due to wave breaking. Then the wave breaking initiation and cessation criterion based on the FSA, Kennedy et al. [3], is presented and finally the new criterion based on the RTFN, Okamoto and Basco [10].

2.5.1 Eddy viscosity

To model the turbulent mixing and dissipation caused by breaking, an "eddy viscosity" approach is used. It consists in adding an ad-hoc dissipative and momentum conservative term R_b to the momentum equation. This term contains the eddy viscosity.

$$R_b = \frac{1}{h+\eta}\frac{\partial}{\partial x}\left(\nu_e \frac{\partial}{\partial x}\left[(h+\eta)u\right]\right) \tag{7}$$

and ν_e is the eddy viscosity and $h+\eta$ represents the total water depth. The eddy viscosity is defined in agreement with experimental data as:

$$\nu_e = B.\delta_b^2.H.\left|\frac{\partial \eta}{\partial t}\right| \tag{8}$$

where δ_b is the mixing length coefficient and $H = h+\eta$ is the total water depth.

The purpose of the parameter B is to avoid an impulsive start of the wave breaking and consequently the instability of the solution. The B parameter is defined as follows in a simple linear growth from zero to one:

$$B = \begin{cases} 1 & \text{if } \dfrac{\partial \eta}{\partial t} \geq 2.\dfrac{\partial \eta^*}{\partial t} \\ \dfrac{\partial \eta/\partial t}{\partial \eta^*/\partial t} - 1 & \text{if } \dfrac{\partial \eta^*}{\partial t} < \dfrac{\partial \eta}{\partial t} \leq 2.\dfrac{\partial \eta^*}{\partial t} \\ 0 & \text{if } \dfrac{\partial \eta}{\partial t} \leq \dfrac{\partial \eta^*}{\partial t} \end{cases} \tag{9}$$

2.5.2 Free Surface Elevation Acceleration (FSA) Criterion

This criterion is used in a number of Boussinesq models such as FUNWAVE, Kennedy et al. [3]. The control parameter of this model is the free surface elevation acceleration criterion. To control the critical condition three parameters are needed.

A breaking event begins when $\partial\eta/\partial t$ exceeds an initial threshold value and it will continue even if $\partial\eta/\partial t$ drops below that value. This threshold is given by $\partial\eta^*/\partial t$ and determines the onset and the cessation of wave breaking. The use of $\partial\eta/\partial t$ as an initiation parameter ensures that the dissipation is concentrated in the front face of the wave as happens in nature. The magnitude of the threshold value will decrease in time from the initial value $\partial\eta^{(I)}/\partial t$ to the final value $\partial\eta^{(F)}/\partial t$. A simple linear relation is used to model the evolution of $\partial\eta^*/\partial t$:

$$\frac{\partial\eta^*}{\partial t}=\begin{cases}\dfrac{\partial\eta^{(I)}}{\partial t} & \text{if } t-t_0\le 0\\ \dfrac{\partial\eta^{(F)}}{\partial t} & \text{if } t-t_0\ge T^*\\ \dfrac{\partial\eta^{(I)}}{\partial t}+\dfrac{t-t_0}{T^*}\left(\dfrac{\partial\eta^{(F)}}{\partial t}-\dfrac{\partial\eta^{(I)}}{\partial t}\right) & \text{if } 0\le t-t_0<T^*\end{cases} \tag{10}$$

where T^* is the transition time, t_0 is the instant where breaking was initiated and so $t-t_0$ is the age of the wave breaking event. The expressions for $\partial\eta^{(I)}/\partial t$, $\partial\eta^{(F)}/\partial t$ and T^* are:

$$\frac{\partial\eta^{(I)}}{\partial t}=ini*\sqrt{g.H_a}\ ,\ \frac{\partial\eta^{(F)}}{\partial t}=fin*\sqrt{g.H_a}\ ,\ T^*=tcst*\sqrt{H_a/g} \tag{11}$$

where ini, fin and tcst must be calibrated for each case. Recommended values from Kenedy *et al.* [3] are ini=0.65, fin=0.15 and Tcst= 5.

2.5.3 Relative Trough Froude Number (RTFN) criterion

The Relative Trough Froude Number (RTFN) was introduced by Utku [14] as a wave breaking index under the moving hydraulic jump concept. The definition equation of the RTFN was modified by Okamoto and Basco [10] as follows:

$$Fr_t=\frac{C_{crest}-u_{trough}}{C_{trough}} \tag{12}$$

where *C* is wave celerity and u is particle velocity. Subscripts denote the location in the wave. Wave breaking begins when the RTFN exceeds a critical value and ceases when it becomes lower than the critical value.

Uktu and Basco [15] conducted a series of experiments and confirmed that the critical condition of RTFN at the beginning of a breaking event is consistent for various conditions of incident wave. The most important feature of the RTFN theory is that it realizes wave breaking with only one coefficient.

The implementation of RTFN formulation into the one dimensional model BOUSS3W followed the procedure carried out by Okamoto [9] for regular waves, namely:

- Determination of the location of the through and the crest, using a fixed-length window that moves along the computational domain;
- Calculation of the phase-resolved characteristics of the wave (particle velocity, wave speed in through and the crest), based on the model results;
- Calculation of the RTFN value;
- Comparison of the RTFN value with the critical Froude number. If RTFN exceeds the critical value, the turbulent viscosity term due to wave breaking is added to the Boussinesq equation at all nodes from the crest to the trough.

3 APPLICATIONS

The model was applied to a simple case of wave propagation and breaking of regular waves over a constant slope beach profile for which there are experimental results obtained by Hansen and Svendsen, [2].

The calculations were performed for the two wave breaking formulations. For each formulation, the methodology was as follows:

- A calibration of the wave breaking parameters is performed by using one of the test conditions used on the experiments performed by Hansen and Svendsen;
- Once the best parameters were defined, the numerical model is applied to the other test conditions of the same experiment.
- Comparisons with experimental and numerical results were made using three statistical parameters: the agreement index, AI (Willmott et al. [19]), Equation 14, the quadratic mean error (RMSE) and the absolute mean error (BIAS), each given by equations:

$$AI = 1 - \frac{\sum_{i=1}^{n} |y_i - x_i|^2}{\sum_{i=1}^{n} \left(|y_i - \bar{x}| + |x_i - \bar{x}| \right)^2}, \quad BIAS = \frac{\sum_{i=1}^{n} (y_i - x_i)}{N} \text{ and } RMSE = \sqrt{\frac{\sum_{i=1}^{n} (y_i - x_i)^2}{N}} \tag{13}$$

where xi are the experimental values, yi are the numerical model values, $\bar{x}$ is the average experimental value and N is the number of points. The agreement index ranges from 0 to 1, being 1 the maximum agreement between experimental and numerical values.

The numerical simulations were run in a PC with a dual Intel® CoreTM Quad CPU Q6600 at 2.4Ghz and 1.97GB RAM memory.

3.1 Constant Slope Beach

Waves are generated at a 0.36m depth and shoal on a 1:34.26 slope until they break, Fig. 1 Test cases number 031041 and 051041 from Hansen and Svendsen [2] experiments were reproduced in this work which correspond to the wave characteristics Table 1.

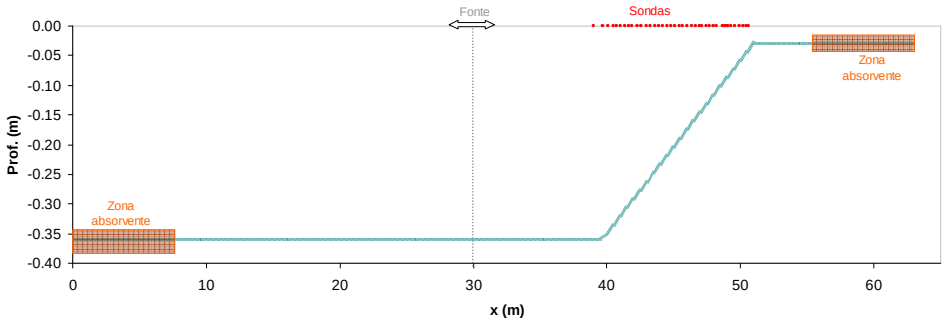

Fig. 1 - Bathymetry and location of source, sponge layers and wave gauges.

Test	Period (s)	Wave Height (cm)
031041	3.33	4.30
051041	2.00	3.60

Table 1 - Characteristics of generated waves.

The simulation time was of 40 s. The numerical domain has 63 m in length and the source is located at x=30.0 m. Two sponge layers were placed at the extremities. The domain was discretized with 4816 finite elements with 0.098 m spacing between nodes. Over the slope 35 wave gauges were placed to measure wave heights. In order to avoid numerical instabilities the viscosity parameter was 3.0×10^{-3}, for cases 031041 and 2.2×10^{-3} for case 051041.

3.1.1 Parameter calibration of RTFN criterion

In this case, the calibrated parameter is the critical Froude number Frc. This parameter was set to values between 1.25 and 1.47. Tests 031041 and 051041 were simulated and an error statistical analysis was performed. The results of this calibration are presented in Fig. 2, and Fig. 3 and the statistical analysis is presented in Table 2.

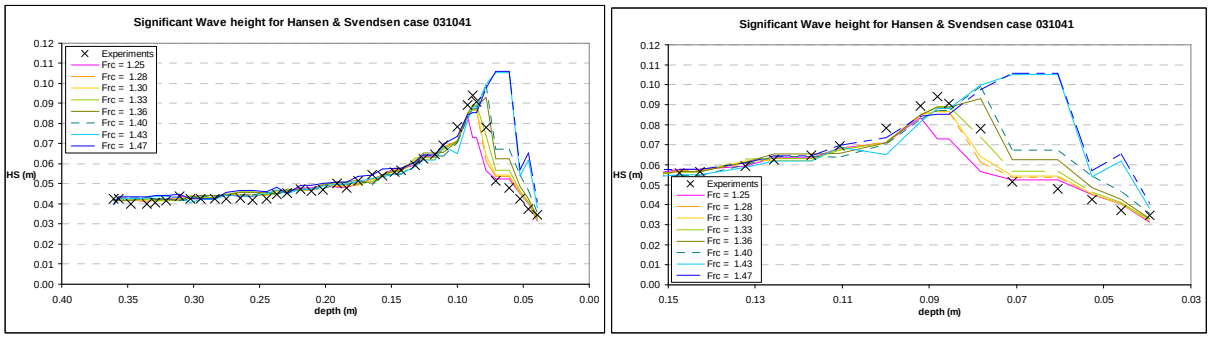

Fig. 2 - Calibration of critical Froude number for test 031041.

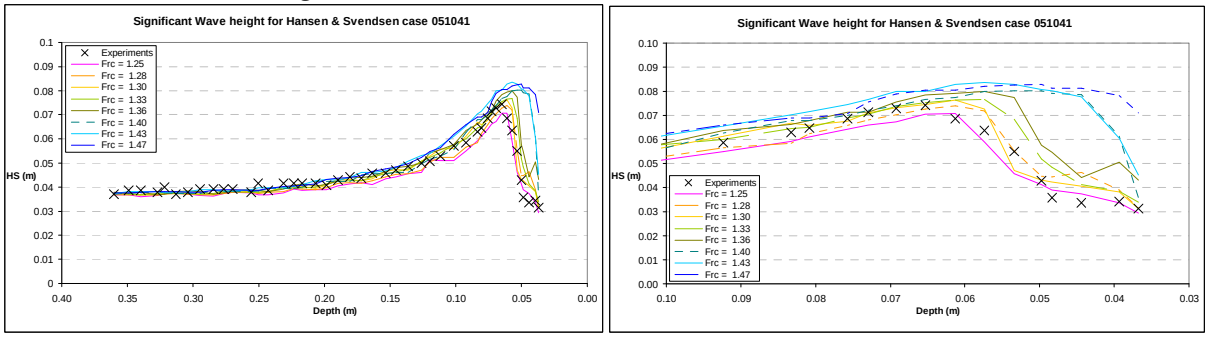

Fig. 3 - Calibration of critical Froude number for test 051041.

Frc	*Test 031041*			*Test 051041*		
	BIAS	*RMSE*	*AI*	*BIAS*	*RMSE*	*AI*
1.25	-0.0013	0.0059	94.68%	-0.0024	0.0040	96.78%
1.28	-0.0004	0.0036	98.26%	-0.0007	0.0043	96.36%
1.30	-0.0004	0.0034	98.46%	**0.0003**	**0.0030**	**98.40%**
1.33	**0.0004**	**0.0030**	**98.89%**	0.0011	0.0042	96.99%
1.36	0.0014	0.0046	97.47%	0.0030	0.0069	92.62%
1.40	0.0015	0.0063	95.30%	0.0045	0.0126	78.59%
1.43	0.0037	0.0139	80.18%	0.0065	0.0133	78.29%
1.47	0.0052	0.0142	79.38%	0.0072	0.0156	71.65%

Table 2 – Error statistics for different critical Froude numbers for tests 031041 and 051041.

Results show that the critical Froude number is a sensitive parameter and determines the accuracy of the simulation in the wave breaking zone and especially after wave breaks. The energy dissipation that occurs after the break is strongly influenced by the location of the first breaking points. Therefore a correct estimation of this parameter is highly important. For the first test a critical Froude number of 1.33 produced the best fit to the experimental results, for the second test a critical Froude number of 1.30 produced the best fit. This shows that this parameter also is sensitive to the wave characteristics.

3.1.2 Results

Fig. 4 to Fig. 5 present the numerical and experimental results obtained for the incident wave conditions: 031041 and 051041, considering the two formulations. Calibration of the parameters of the FSA method was done in Pinheiro et al [11] and the values adopted here were ini=0.85, fin=0.15 and Tcst= 5 for 031041 test and ini=0.90, fin=0.15 and Tcst= 5 for 051041 test.

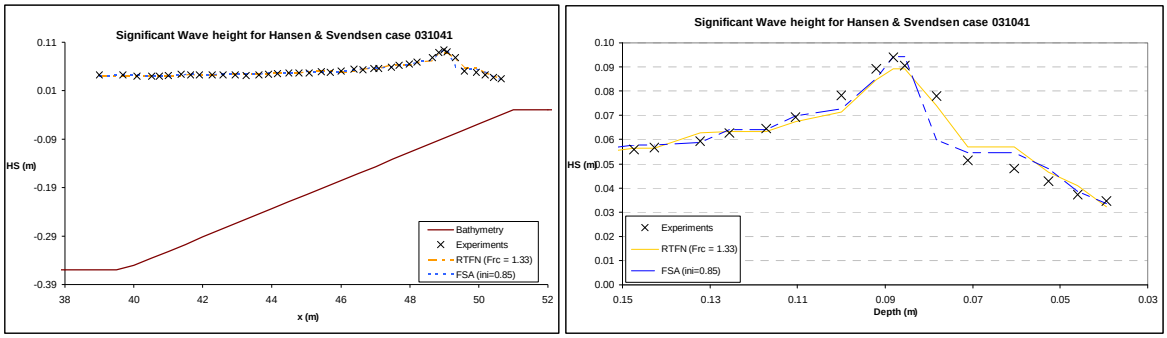

Fig. 4 - Significant wave heights HS (m) over the bathymetry for test case 031041. Comparison of Kennedy's and RTFN criterions.

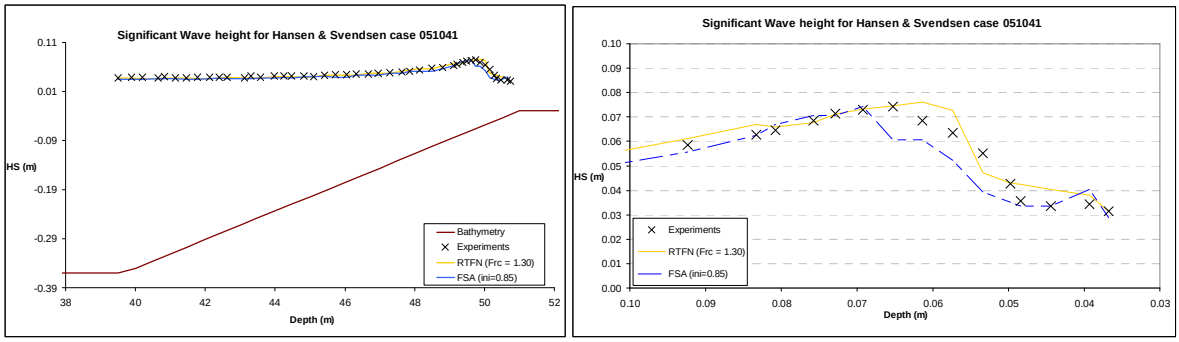

Fig. 5 - Significant wave heights HS (m) over the bathymetry for test case 051041. Comparison of Kennedy's and RTFN criterions.

In general, for all cases tested and breaking formulations, the numerical results do follow the experimental values, before and after breaking takes place. Indeed, for each test case, the wave height grows due to decreasing depth and breaks at the same locations obtained in experimental tests. After wave breaking occurs, the wave height decreases due to energy dissipation resulting from the turbulent phenomenon.

Table 3. Error statistics for Kennedy's and RTFN criterions for tests 031041 and 051041.

	Test 031041			*Test 051041*		
	BIAS	RMSE	AI	BIAS	RMSE	AI
FSA (ini=0.85, 0.90)	0.0004	0.0037	98.32%	-0.0030	0.0048	95.64%
RTFN (Frc=1.33, 1.30)	0.0004	0.0030	98.89%	0.0003	0.0030	98.40%

The comparison of the two wave breaking criteria shows that:

- The wave height before wave breaking is well simulated by the model;
- The wave breaking positions is well captured with both models.
- The energy dissipation after wave breaking is very well simulated with both criterions especially with the new criterion.

3.2 Barred Beach

BOUSS3W was applied to one of the experimental test cases described in Sancho *et al.* [13], in a 100 m long, 3 m wide and 5 m depth channel of Polytechnic University of Catalunha. A regular wave of 0.112 m high and 2.5 s period was simulated which corresponds to Test A.

The bathymetry is shown in Fig. 6 and the depth varies from -2.05 m and -0.012 m.

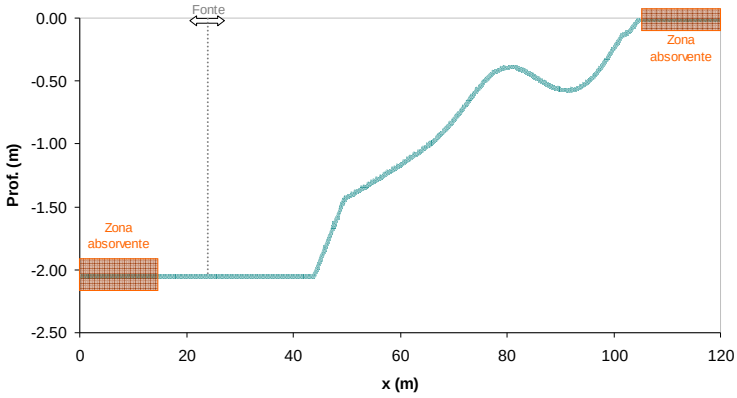

Fig. 6 – Barred beach Bathymetry. Source location and sponge layers.

The source function is located at x=26 m. Two sponge layers were placed at both ends of the domain. Node spacing is of 0.05 m in a total of 2393 nodes. Total simulation time was 70 s. 43 numerical probes were placed over the bar and the beach to measure significant wave heights.

3.2.1 Parameter calibration of RTFN criterion

The critical Froude number F*rc* was set to values between 1.25 and 1.47. Error statistical analysis was performed. The results of this calibration are in Fig. 2, and the statistical analysis is presented in Table 2.

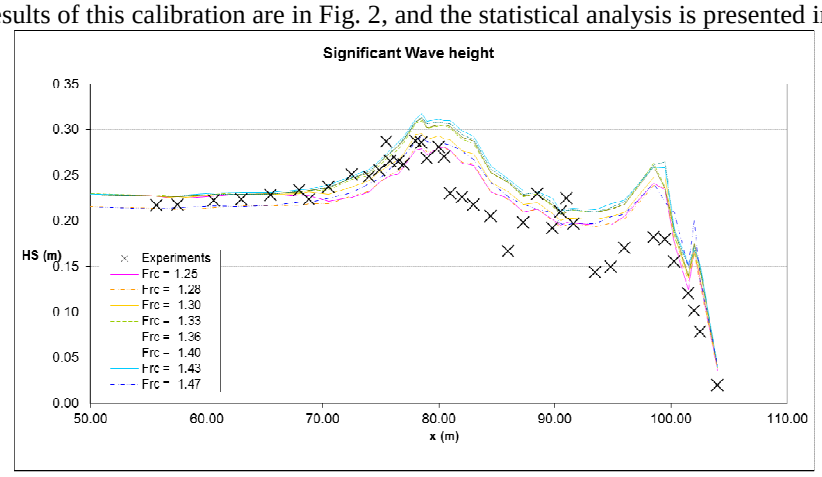

Fig. 7 - Calibration of critical Froude number for the bared beach test A.

Frc	*Test 031041*		
	BIAS	*RMSE*	*AI*
1.25	0.0116	0.0298	91.86%
1.28	**0.0100**	**0.0295**	**92.01%**
1.30	0.0199	0.0335	90.52%
1.33	0.0271	0.0385	88.47%
1.36	0.0282	0.0394	88.00%
1.40	0.0303	0.0418	86.68%
1.43	0.0323	0.0431	86.20%
1.47	0.0164	0.0344	89.08%

Table 4 – Error statistics for different critical Froude numbers for the bared beach test A.

Results show that the critical Froude number is a sensitive parameter and determines the accuracy of the simulation in the wave breaking zone and especially when several breaks occur. The energy dissipation is strongly influenced by the location of the first breaking point which depends on the Frc, however, the second break is well captured with almost all the Frc simulated. Therefore a correct estimation of this parameter is highly important. For the constant slope beaches shown in section 3.1 critical Froude numbers of 1.33 and 1.30

produced the best fit to the experimental results, in this case a critical Froude number of 1.28 produced the best fit. The energy recovery that takes place over the through of the bar is not captured by the model that is why the second break occurs with an overestimated wave height.

3.2.2 Results

Fig. 8 present the numerical and experimental results obtained for the incident wave conditions of test A of the bared beach experimental case, considering the two formulations and additionally the results of numerical model FUNWAVE.

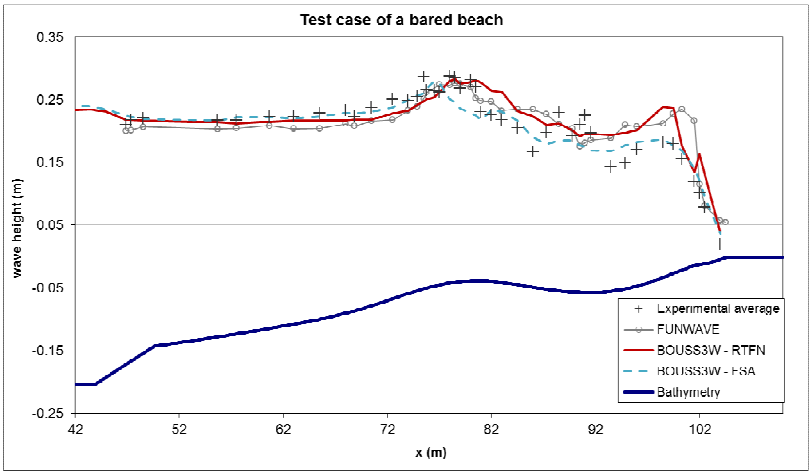

Fig. 8 – Barred beach wave breaking results.

In general the numerical results do follow the experimental values, before and after the first breaking takes place and also before and after the second breaking takes place. None of the numerical models were able to capture the energy recovery after the bar, but the second breaking event is well reproduced.

Table 5. Error statistics for Kennedy's and RTFN criterions for the bared beach test A.

	BIAS	RMSE	AI
FUNWAVE	0.0015	0.0300	92.36%
BOUSS3W - FSA	-0.0051	0.0229	95.34%
BOUSS3W - RTFN	0.0271	0.0385	92.01%

From Table 3, it is clear that for this test case the BOUSS3W model with the FSA criterion is closer to the experimental values simulating quite well both breaking events. The RTFN criterion tends to overestimate wave heights. An index of agreement over 92% is achieved by the three simulations which is very good considering the complexity of the wave breaking phenomenon. Nevertheless some adjustments need be implemented to improve the RTFN criterion performance in bared beach profiles.

4 CONCLUSIONS

This paper describes the implementation of wave breaking physical process in the BOUSS-WMH model by using two wave breaking formulations, Kennedy et al. [3] and Okamoto and Basco [10].

The validation was performed with two test conditions of Hanssen and Svendsen [2] experiments and one test condition of Sancho *et al.* [13] experiments. Comparison between experimental data and numerical results for both formulations was made and showed that the wave breaking physical process introduced was adequately implemented in the model and there is a very good agreement with measured data. The energy dissipation after wave breaking is very well simulated with the new RTFN criterion in a constant slope beach profile. However, in a bared beach profile, the RTFN criterion didn't perform as well as the FSA criterion. Therefore, more tests need to be done to assess this method's ability to simulate wave breaking over different types of beach profiles. The influence of bottom friction must be studied as well.

5 AKNOWLEGMENTS

Financial support from the "Fundação para a Ciência e Tecnologia" (FCT) of the Ministry of Science and High Education of Portugal, through projects PTDC/ECM/73145/2006, PTDC/ECM/67411/2006 and PRDC/AAC-AMB/12072/2010 are gratefully acknowledged.

REFERENCES

1. Antunes do Carmo J.S. & Seabra Santos F.J. On breaking waves and wave-current interaction in shallow water: a 2DH finite element model International Journal for Numerical Methods in Fluids, vol. 22, 429-444
2. Hansen, J. Buhr & I.A. Svendsen. Regular waves in shoaling water. Experimental data. Series Paper No 21, Inst. Hydrodyn. and Hydraulic Engrg., Techn. Univ. of Denmark, 1979, 20 + 223 pp.
3. Kennedy A. B., Chen Q., Kirby J. T., Dalrymple R. A. Boussinesq Modeling of Wave Transformation, Breaking, and Runup. I: 1D. J. Waterway, Port, Coastal, and Ocean Eng. P. 39-47, 2000.
4. Kirby J.T., Wei G. And Chen Q. FUNWAVE 1.0 Fully nonlinear Boussinesq wave model. Documentation and user's manual. UD, Newark, Rel.CACR 98 06, September 1998
5. Le Roux, J.P., (2001). A simple method to predict the threshold of particle transport under oscillatory waves. Sedimentary Geology 143 (2001): 59–70—Reply to discussion
6. Li Y.S., Liu S.-X., Yu Y.-X. And Lai G.-Z. Numerical modeling of Boussinesq equations by a finite element method. Coastal Engineering, vol. 37, 97-122, 1999
7. Nwogu, O. & Demirbilek, Z. (2001) BOUSS-2D: A Boussinesq Wave Model for Coastal Regions and Harbors. Report 1 Theoretical Background and User.s Manual, ERDC/CHL TR-01-25, U.S. Army Corps of Engineers
8. Nwogu, O. (1993) Alternative form of Boussinesq equations for near-shore wave propagation. J. Waterway, Port, Coastal, and Ocean Engineering. 119, 6, pp. 618 - 638.
9. Okamoto, T. (2003). Boussinesq Model and the relative trough Froude Number (RTFN) for wave breaking. PhD Thesis. Old Dominion University Okamoto et al 2004
10. Okamoto, T., Basco, D. R. (2006). The Relative Trough Froude Number for Initiation of Wave Breaking: Theory, Experiments and Numerical Model Confirmation, Coastal Eng., 53, 675-690.
11. Pinheiro L. V., Rodriguez, V., Fortes C. J. E. M., Fernandes J. L. M. (2011) Desempenho do modelo BOUSS3W na rebentação de ondas. Congresso de Métodos Numéricos em Engenharia 2011. Coimbra, 14 a 17 de Junho. (in portuguese)
12. Pinheiro L.V., Virginie Rodriguez, Fortes C. J., Teixeira P.R., Walkley M.A. BOUSS-WMH Nonlinear Wave Propagation Model. Bottom Friction Implementation. 7th European Conference on Computational Fluid Dynamics ECCOMAS CFD 2010 Lisbon, Portugal, 14–17 June 2010.
13. Sancho F.E, P.A. Mendes, J.A Carmo, M.G. Neves, G.R. Tomasicchio, R. Archetti, L. Damiani, M. Mossa, A. Rinaldi, X. Gironella e A. Sanchez-Arcilla "Wave hydrodynamics over a barred beach", Proc. 4th Int. Symp. on Ocean Wave Measurement and Analysis - Waves 2001, S. Francisco, ASCE, 1170-1179. (2001)
14. Utku, M. (1999) - The Relative Trough Froude Number: A New Wave Breaking Criteria', Ph.D. Dissertation, Dept. of Civil and Environmental Engr., Old Dominion University, Norfolk, Virginia.
15. Utku, M., Basco, D.R. (2002). A New Criteria for Wave Breaking Based on the Relative Trough Froude Number. Proc. of 28th ICCE, (Wales), ASCE, New York, 258-268.
16. Walkley M. & Berzins M. A Finite element method for the two-dimensional extended Boussinesq equations International journal for numerical methods in fluids, vol. 39, no.2, 865-885, 2002.
17. Walkley M. A (1999) Numerical Method for Extended Boussinesq Shallow-Water Wave Equations. PhD Thesis, The University of Leeds School of Computer Studies
18. Wei, G., Kirby, J. T. and Sinha, A., 1999. Generations of waves in Boussinesq models using a source function method. Coastal Engineering, 36(4), 271-299.
19. Willmott, C.J., S.G. Ackleson, R.E. Davis, J.J. Feddema, K.M. Klink, D.R. Legates, J. O'Donnell e C.M. Rowe (1985) Statistics for the evaluation and comparison of models. Journal of Geophysical Research, 90 (c5), p. 8995-9005